Novel Animal Model of Crumbs-Dependent Progressive Retinal Degeneration That Targets Specific Cone Subtypes

Jinling Fu,[1,2] Mikiko Nagashima,[3] Chuanyu Guo,[2] Pamela A. Raymond,[3] and Xiangyun Wei[2,4–6]

[1]Department of Ophthalmology, the Second Hospital of Jilin University, Changchun, Jilin, China
[2]Department of Ophthalmology, University of Pittsburgh School of Medicine, Pittsburgh, Pennsylvania, United States
[3]Department of Molecular, Cellular, and Developmental Biology, College of Literature, Science, and the Arts, University of Michigan, Ann Arbor, Michigan, United States
[4]Department of Developmental Biology, University of Pittsburgh, School of Medicine, Pittsburgh, Pennsylvania, United States
[5]Department of Microbiology and Molecular Genetics, University of Pittsburgh, School of Medicine, Pittsburgh, Pennsylvania, United States
[6]Louis J. Fox Center for Vision Restoration, University of Pittsburgh, School of Medicine, Pittsburgh, Pennsylvania, United States

Correspondence: Xiangyun Wei, Department of Ophthalmology, University of Pittsburgh School of Medicine, 3501 Fifth Avenue, Pittsburgh, PA 15213, USA; weix@upmc.edu.
Pamela A. Raymond, Department of Molecular, Cellular, and Developmental Biology, College of Literature, Science, and the Arts, University of Michigan, 3003 Kraus Natural Science Building, 830 North University Avenue, Ann Arbor, MI 48109-1048, USA; praymond@umich.edu.

JF and MN contributed equally to the work presented here and should therefore be regarded as equivalent authors.

Submitted: July 7, 2017
Accepted: December 10, 2017

Citation: Fu J, Nagashima M, Guo C, Raymond PA, Wei X. Novel animal model of Crumbs-dependent progressive retinal degeneration that targets specific cone subtypes. *Invest Ophthalmol Vis Sci*. 2018;59:505–518. https://doi.org/10.1167/iovs.17-22572

Purpose. Human *Crb1* is implicated in some forms of retinal degeneration, suggesting a role in photoreceptor maintenance. Multiple *Crumbs* (*Crb*) polarity genes are expressed in vertebrate retina, although their functional roles are not well understood. To gain further insight into Crb and photoreceptor maintenance, we compared retinal cell densities between wild-type and *Tg(RH2-2:Crb2b-sf^{EX}/RH2-2:GFP)^{pt108b}* transgenic zebrafish, in which the extracellular domain of Crb2b-short form (Crb2b-sf^{EX}) is expressed in the retina as a secreted protein, which disrupts the planar organization of RGB cones (red, green, and blue) by interfering with Crb2a/2b-based cone-cone adhesion.

Methods. We used standard morphometric techniques to assess age-related changes in retinal cell densities in adult zebrafish (3 to 27 months old), and to assess effects of the Crb2b-sf^{EX} transgene on retinal structure and photoreceptor densities. Linear cell densities were measured in all retinal layers in radial sections with JB4-Feulgen histology. Planar (surface) densities of cones were determined in retinal flat-mounts. Cell counts from wild-type and *pt108b* transgenic fish were compared with both a "photoreceptor maintenance index" and statistical analysis of cell counts.

Results. Age-related changes in retinal cell linear densities and cone photoreceptor planar densities in wild-type adult zebrafish provided a baseline for analysis. Expression of Crb2b-sf^{EX} caused progressive and selective degeneration of RGB cones, but had no effect on ultraviolet-sensitive (UV) cones, and increased numbers of rod photoreceptors.

Conclusions. These differential responses of RGB cones, UV cones, and rods to sustained exposure to Crb2b-sf^{EX} suggest that Crb-based photoreceptor maintenance mechanisms are highly selective.

Keywords: retinal cell density, retinal degeneration, photoreceptor degeneration, retinitis pigmentosa, Leber's congenital amaurosis, Crumbs

The maintenance of vertebrate retinal photoreceptors is critical for normal vision because photoreceptors normally persist for the entire life span; if they degenerate in mammals, they cannot be replenished. However, understanding mechanisms of photoreceptor maintenance is challenging because photoreceptor degeneration and retinal dystrophy are linked to dozens of genes, including the *Crumbs* (*Crb*) family.[1–3] For example, pathogenic mutations of human *Crumbs 1 (CRB1)* cause severe retinal dystrophies, accounting for 5% of retinitis pigmentosa (RP) and 10% of Leber's congenital amaurosis (LCA).[4–9] Despite the relative prevalence of CRB1-based RP and LCA, the molecular etiology of CRB1 in photoreceptor degeneration is not understood.[10]

Crb proteins are Type I transmembrane proteins that regulate apicobasal epithelial polarity[11,12] and cell-cell adhesion.[13] In the retina, Crb proteins control epithelial polarity and apical membrane size of photoreceptors in both *Drosophila* and vertebrates.[4,14–16] A single *Crb* gene exists in the fly, but in mammals, three homologs, *Crb1*, *Crb2*, and *Crb3,* are expressed in photoreceptors and/or Müller glia in the retina.[10,17–20] In zebrafish retina, *crb1*, *crb2a*, and *crb2b* gene homologs are expressed, and two transcriptional start sites in the *crb2b* gene yield two proteins, Crb2b-long form (Crb2b-lf), and Crb2b-short form (Crb2b-sf), that differ in length of their extracellular domain.[21–23]

To gain insight into potential Crb functions in photoreceptor maintenance, we first analyzed retinal cell densities as a function of age in wild-type zebrafish to provide a baseline for evaluating the effects of genetic abnormalities in *Crb* on photoreceptor maintenance. To our knowledge, this is the first comprehensive analysis of retinal cell densities in zebrafish, although similar studies have been conducted in other teleost species.[24–27] We then compared photoreceptor densities in wild-type with those in the transgenic zebrafish *Tg(RH2-*

2:Crb2b-sf^{EX}/RH2-2:GFP)^{pt108b} (subsequently referred to as *pt108b*). In *pt108b*, blue cones (and less frequently, rods and green cones) secrete Crb2b-sf^{EX} (the extracellular domain of Crb2b-short form), which interrupts Crb2a/2b-mediated adhesion among RGB cones (red, green, and blue cones) by competitively binding to the extracellular domains of endogenous Crb2a and Crb2b.[22] Although the inhibition of Crb-mediated cone-cone adhesion disrupts the planar spatial patterning of cones, and destroys the regular lattice arrangement of the cone mosaic,[22] it is unclear whether or not photoreceptor maintenance is affected. Here we report differential effects on maintenance of rods, RGB cones, and UV cones after interference with Crb-based adhesion.

Materials and Methods

Zebrafish Care

AB and TL wild-type, and *Tg(RH2-2:Crb2b-sf^{EX}/RH2-2:GFP)^{pt108b}* transgenic zebrafish[22] were maintained in a 14-hour light and 10-hour dark cycle with standard husbandry procedures. All animal protocols conformed to regulations at the University of Pittsburgh and the University of Michigan as well as to the ARVO Statement for the Use of Animals in Ophthalmic and Vision Research.

Immunohistochemistry

To verify photoreceptor subtypes in *pt108b* fish, we performed immunohistochemistry with the following primary and secondary antibodies: rabbit polyclonal anti-UV opsin for UV cone outer segments (gift from David Hyde, PhD),[28] anti-Zpr1 for green/red double cones (ZFIN), Cy3-conjugated goat anti-mouse IgG (Catalog no. 115-165-166; Jackson ImmunoResearch Labs, Jackson, PA, USA), and Cy5-conjugated donkey anti-rabbit IgG (Catalog no. 711-175-152; Jackson ImmunoResearch Labs). Images were collected with a Fluoview FV1000 confocal microscope (Olympus, Tokyo, Japan).

JB4 Plastic Sectioning and Feulgen Staining

Zebrafish eyes were fixed in 4% paraformaldehyde in PBS at room temperature overnight. The fixed samples were dehydrated in alcohol and embedded in JB4 resin (JB4 embedding kit; Polysciences, Inc., Warrington, PA, USA), following the manufacturer's protocol. The samples were sectioned at 3-μm thickness with a Shandon Finesse microtome (Thermo Electron Co., Waltham, MA, USA). Plastic sections were collected on glass slides, stained with the Feulgen reaction to visualize the cell nuclei,[29] observed under an Olympus UPlanSApo ×20/0.80 oil objective (Olympus BX60 microscope), and photographed with a SPOT RT camera, software version 4.6 (Diagnostic Instruments, Inc., Sterling Heights, MI, USA).

Evaluating Linear Retinal Cell Densities

We define "linear cell density" as the number of cells of a given subtype counted in a curved segment of retina aligned with the retinal layers in a radial section through the center of the eye. To evaluate cell densities across the retina in Feulgen-stained sections, eyes were sectioned radially in either dorsal-ventral or nasal-temporal (anterior-posterior) planes (Fig. 1A; Supplementary Fig. S1); three consecutive sections through the retinal center were collected and divided into five local regions with an angular subtense of 36 degrees: two peripheral regions, two intermediate regions, and one central region (Fig. 1B). The newly generated tissue in the growing marginal regions (approximately 100 μm) was excluded from quantification (Fig. 1B, black areas). Thus, retinas were systematically sampled at nine local regions representing the midline regions of four retinal quadrants: nasal, dorsal, temporal, and ventral (Fig. 1C).

In each sampling region, to determine the linear cell density, we counted cell nuclei in a retinal segment of 200 μm in length parallel to cellular layers (Fig. 1B). Retinal cells were quantified into six categories according to nuclear morphology and position (Figs. 1D–F): retinal ganglion cells (nuclei localized to the basal layer of the retina), basal inner nuclear layer cells (including amacrine cells, Müller cells, and bipolar cells), horizontal cells (nuclei horizontally elongated and localized to the most apical tier of the inner nuclear layer), rods (nuclei round and more densely stained than cone nuclei, and localized to the basal half of the outer nuclear layer), UV cones (nuclei also rounded but larger and stained lighter than rods, localized apical to rod nuclei and basal to the outer limiting membrane [OLM], and regularly separated from each other), and RGB cones (nuclei elongated in the apicobasal direction, stained lighter than rod nuclei, and localized largely apical to the OLM). Five eyes were sampled for each age and each local region; cell nuclei in three consecutive radial retinal sections were counted and averaged. We performed a paired *t*-test and ANOVA with post hoc Tukey statistical tests, using JMPPro 12.0.1 (SAS Institute, Inc., Cary, NC, USA) to compare cell densities between different conditions.

Evaluating Planar Cone Densities by Flat-Mount Imaging

We define "planar cone density" as the number of cones contained within a unit of surface area in a retinal flat-mount. Retinal flat-mount immunohistochemistry was performed as previously described.[30] In brief, dark-adapted retinas were dissected and flattened with radial relaxing cuts including a large ventral cut, fixed at 4°C overnight in 4% paraformaldehyde in 0.1M phosphate buffer with 5% sucrose, then processed for immunohistochemistry. Primary and secondary antibody incubations were at the following dilutions: mouse anti-ZO-1A-12 (Invitrogen, Camarillo, CA, USA), 1:200; rabbit anti-active Caspase-3 Clone C92–605 (RD Biosciences, San Jose, CA, USA), 1:1000; Dylight 550-conjugated anti-mouse IgG (Thermo Scientific, Waltham, MA, USA), 1:200; and DyLight 650-conjugated anti-rabbit IgG (Thermo Scientific), 1:200. Antigen retrieval in 10-mM sodium citrate with 0.05% Tween20 (pH 6.0) was performed for ZO-1 staining.[30] Images were captured with a Zeiss Axio Image ZI epifluorescent microscope (Carl Zeiss Microimaging, Inc., Thornwood, NY, USA) with an ApoTome module for optical sectioning using structured illumination. Images were processed for two-dimensional (2D) projection (*xy* plane) or three-dimensional (3D) "cut views" (*xz* and *yz* planes) with AxioVision SE64 or Adobe Photoshop CS6 Extended (Adobe Systems, Inc., San Jose, CA, USA).

Cone densities in sampling areas (3087 μm^2) from nine local retinal regions in each of three individual retinas were quantified with Image J (http://imagej.nih.gov/ij/; provided in the public domain by the National Institutes of Health, Bethesda, MD, USA).

Results

Age-Related Changes in Retinal Cell Densities in Wild-Type Zebrafish

To gain insight into Crb functions in photoreceptor maintenance by analyzing *pt108b* effects on the retina, we first need

Investigative Ophthalmology & Visual Science

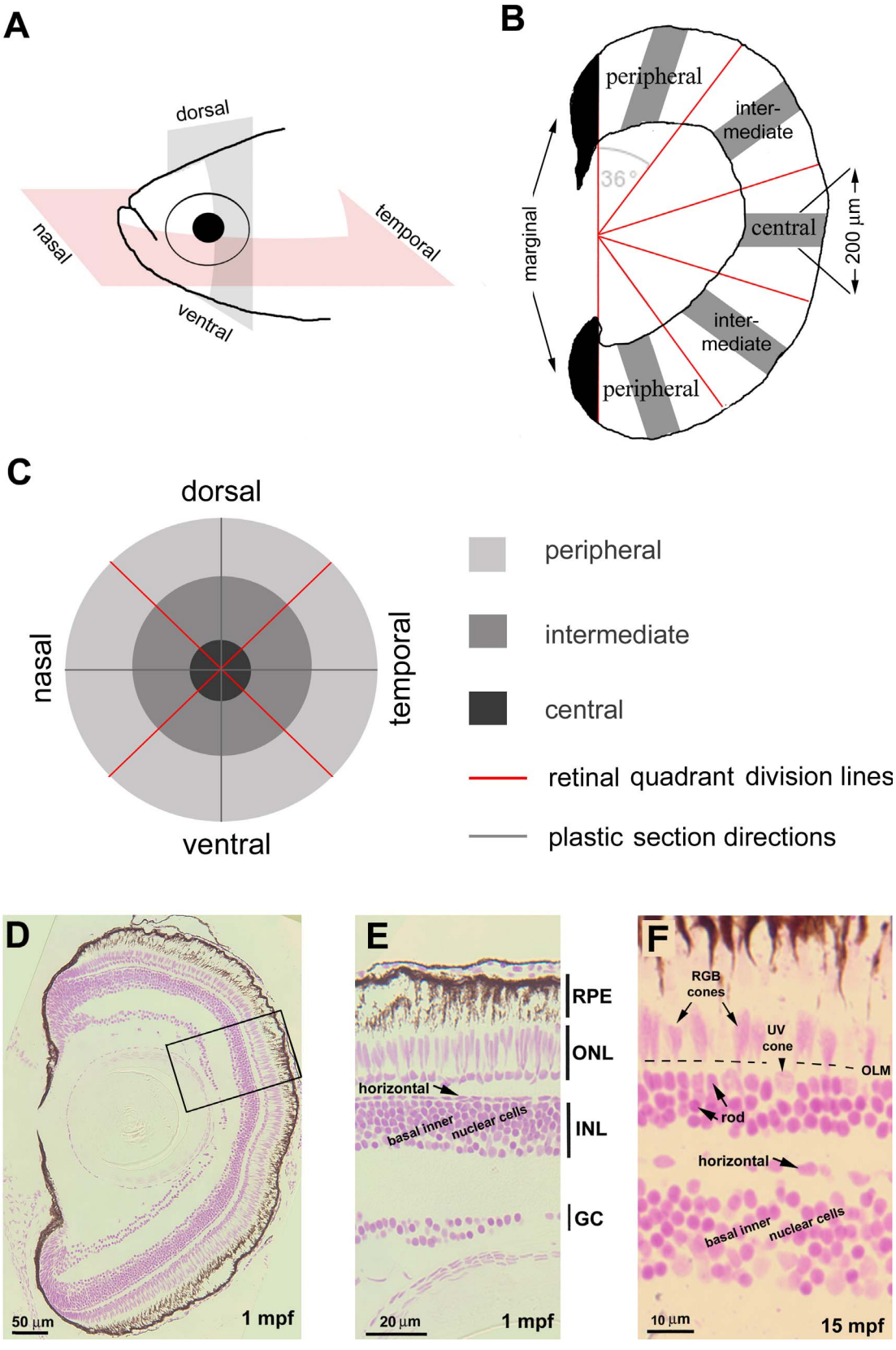

Figure 1. Linear cell densities of six categories of retinal cells were evaluated by JB4-Feulgen histology. (**A**) Zebrafish eyes were sectioned in either the nasal-temporal (anterior-posterior) or ventral-dorsal axis. (**B**) Each retinal section was partitioned by a vertical line to exclude the developing marginal region (*black*) from the differentiated retina, which was further divided into five regions each with angular subtense of 36 degrees. We counted nuclei in 200-µm linear segments (*gray bars*). (**C**) Spatial relationships among the nine sampled retinal regions. (**D–F**) JB4-Feulgen histology illustrates the localization and morphologies of the six retinal cell categories at 1 mpf (**D**, **E**; the *inset box* in **D** outlines the boundary of **E**) and 15 mpf (**F**). The *dashed line* indicates the location of the OLM. GC, ganglion cell layer; INL, inner nuclear layer; ONL, outer nuclear layer.

Investigative Ophthalmology & Visual Science

to understand the effect of normal aging on retinal cell density. Age-related changes in cell densities can be caused by many factors, including cell proliferation, cell death, and compression or stretching of the retina, all of which have been described in association with growth and differentiation of vertebrate retinas.[31–35]

Linear densities of most retinal cell categories in the central region declined progressively by approximately 30% to 40% in adult wild-type zebrafish from 3 mpf (months postfertilization) to 27 mpf (Figs. 2A–F). Correlating with a reduction in linear cell densities, the thickness of the ganglion cell layer was reduced from two to three cells thick at 3 mpf to a single cell layer at 27 mpf (Fig. 2G). Similar trends were also found in the intermediate and peripheral regions (Supplementary Figs. S2–S5). In the central region, UV cone linear densities were not significantly changed, although density declined in other retinal regions (Fig. 2E; Supplementary Figs. S2–S5). Although rod linear density did not show a consistent trend, it was slightly higher in some regions at 15 mpf (Fig. 2D; Supplementary Figs. S2, S4), but otherwise relatively constant.

Topographical Variations of Retinal Cell Densities in Wild-Type Zebrafish

In addition to age-related changes in linear cell density, we discovered topographic variations across the retina, as illustrated in the 3D histogram plots of counts from 15-mpf retinas (Fig. 3). We chose 15 mpf because retinal structure has largely stabilized after the rapid growth in juvenile and young adult stages (3 mpf), but retinal structure has not yet been affected by aging as at 27 mpf (Fig. 2G; Supplementary Fig. S1).

We compared data both within a quadrant radially from central to peripheral, and between quadrants circumferentially across intermediate and peripheral regions. In the radial dimension within a quadrant, linear cell densities tended to decrease from central to intermediate to peripheral in all four quadrants for most retinal cell categories (Supplementary Tables S1, S2), especially ganglion cells (Fig. 3A), horizontal cells (Fig. 3C), UV cones (Fig. 3E), and RGB cones (Fig. 3F), but not basal inner nuclear layer cells (Fig. 3B). In the circumferential dimension (i.e., between quadrants) rod photoreceptor densities vary significantly, and ganglion cells and RGB cones show some variation (Supplementary Table S3). Rod photoreceptor densities in both intermediate and peripheral regions were highest in the dorsal and nasal quadrants (Fig. 3D; Supplementary Tables S1, S3). Conversely, RGB cone density in the ventral intermediate region was higher than in the nasal quadrant (Fig. 3F; Supplementary Tables S1, S3) and retinal ganglion cells showed a trend toward increased density in the ventral and temporal quadrants compared to dorsal (Fig. 3A; Supplementary Tables S1, S3).

We confirmed the topographical variations in a planar cone density analysis of adult 6-mpf retinal flat-mounts, with immunolabeling of ZO1 to reveal the profiles of photoreceptors and Müller glia at the level of OLM. Cone profiles, identified by their shapes, sizes, and stereotypic pattern,[36] were sampled in approximately the same nine local regions defined for the linear cell density analysis (Figs. 1A–C, 4A). The crystalline lattice cone mosaic pattern characteristic of adult zebrafish retina (Fig. 4D–G') is absent in the central region (Fig. 4H), which represents retina that was present in the larval eye.[37] This planar cone density analysis revealed dramatic topographic variations in cone sizes: In particular, in the central region (Fig. 4H) and dorsal quadrant (Figs. 4G, 4G'), UV cones are much larger than RGB cones, and in the ventral quadrant (Figs. 4E, 4E'), all cone profiles are small.

Similar to the linear cone densities, planar cone densities generally decline from central to intermediate to peripheral regions, except in the ventral retina (Figs. 4B, 4C; Supplementary Table S4). Circumferential comparisons between quadrants confirmed that the highest planar cone density was in the ventral intermediate region (Figs. 4B, 4C; Supplementary Table S4). Although we did not count rod profiles in these flat-mount preparations, the higher density of rods in the dorsal region can be appreciated by the accumulation of small, round rod profiles in the spaces between the cones (Fig. 4G' inset; also see Salbreux et al., 2012).[36] Thus, the results of the linear and planar cell density counts both show that cones are denser in ventral retina than in dorsal retina, and rods are denser in dorsal retina than in ventral retina.

Secreted Crb2b-sf^{EX} Has Differential Effects on Photoreceptor Maintenance

In zebrafish, Crb1 is expressed by all cones; Crb2a by cones, rods, and Müller glia; and Crb2b by RGB cones only (Fig. 5A). To gain insight into whether Crb-mediated cone-cone adhesion plays a role in photoreceptor maintenance, we analyzed age-related retinal cell density changes in *pt108b* transgenic fish, in which Crb2b-sf^{EX} is secreted mainly by blue cones, a much more restrictive expression pattern compared with endogenous Crb2a and Crb2b (Fig. 5A; also see Zou et al., 2012).[22] We showed previously that expression of Crb2b-sf^{EX} gradually disrupts the regular alignment of RGB cones into mirror-image pentamers (G-R-B-R-G) by physically interfering with cone-cone adhesions mediated by Crb2a and Crb2b.[22] We reasoned that if Crb2b-sf^{EX} disrupts cone adhesion by physically binding to endogenous Crb proteins, Crb2b-sf^{EX} may also interfere with signaling pathways that might regulate photoreceptor survival via Crb proteins.[10] Comparing flat-mount images of ZO1 cone profiles in 4-mpf young adult pt108b fish with 18-mpf aged adults revealed late-onset disruption of RGB cone spatial organization (Fig. 5B). Importantly, the cone mosaic pattern in 4-mpf pt108b adults is highly organized throughout the retina (Supplementary Fig. S6), with the same topographic variations in cone sizes seen in wild-type adults (Fig. 4), suggesting that Crb2b-sf^{EX} interferes with photoreceptor maintenance, but not cone photoreceptor development.

To quantitatively evaluate whether photoreceptor maintenance is affected in the *pt108* line, we first examined the histologic characteristics of *pt108b* retinas in the central and intermediate regions of aged fish (27 mpf). We found no disruptions in overall retinal lamination in *pt108b*, again consistent with a lack of effect of Crb2b-sf^{EX} on retinal development. However, in the aged adult *pt108b* retinas, very few cone photoreceptor nuclei located apical to the OLM were elongated (Figs. 5C', 5D', 5E'), which is a distinctive characteristic of RGB cone nuclei in the wild-type retina (Figs. 5C–E). In their place were round, lightly stained, and sparsely distributed nuclei (Fig. 5C', arrowheads) that resembled UV cones, whose nuclei normally reside below the OLM in wild-type retina (Fig. 5C, arrowhead). Rod nuclei remained small, round, and darkly stained and localized basal to the OLM in *pt108b* at 27 mpf (Figs. 5C', 5D', 5E'), similar to wild-type retinas (Figs. 5C–E).

We verified cone identities with immunohistochemistry in 27-mpf *pt108b* and found that very few cones expressed arrestin 3a (a regulator of G protein–coupled receptors that is selectively expressed in zebrafish green/red cones and is recognized by the Zpr1 monoclonal antibody), particularly in the central region (Figs. 5D, 5D'). Furthermore, most nuclei of the remaining Zpr1-positive cells had lost their typical elongated morphology and resembled nuclei of UV cones, round and lightly stained (Fig. 5D'; arrow), although most of the cones with round and lightly stained nuclei above the OLM in *pt108b* retinas were UV opsin-positive (Fig. 5D', arrow-

Investigative Ophthalmology & Visual Science

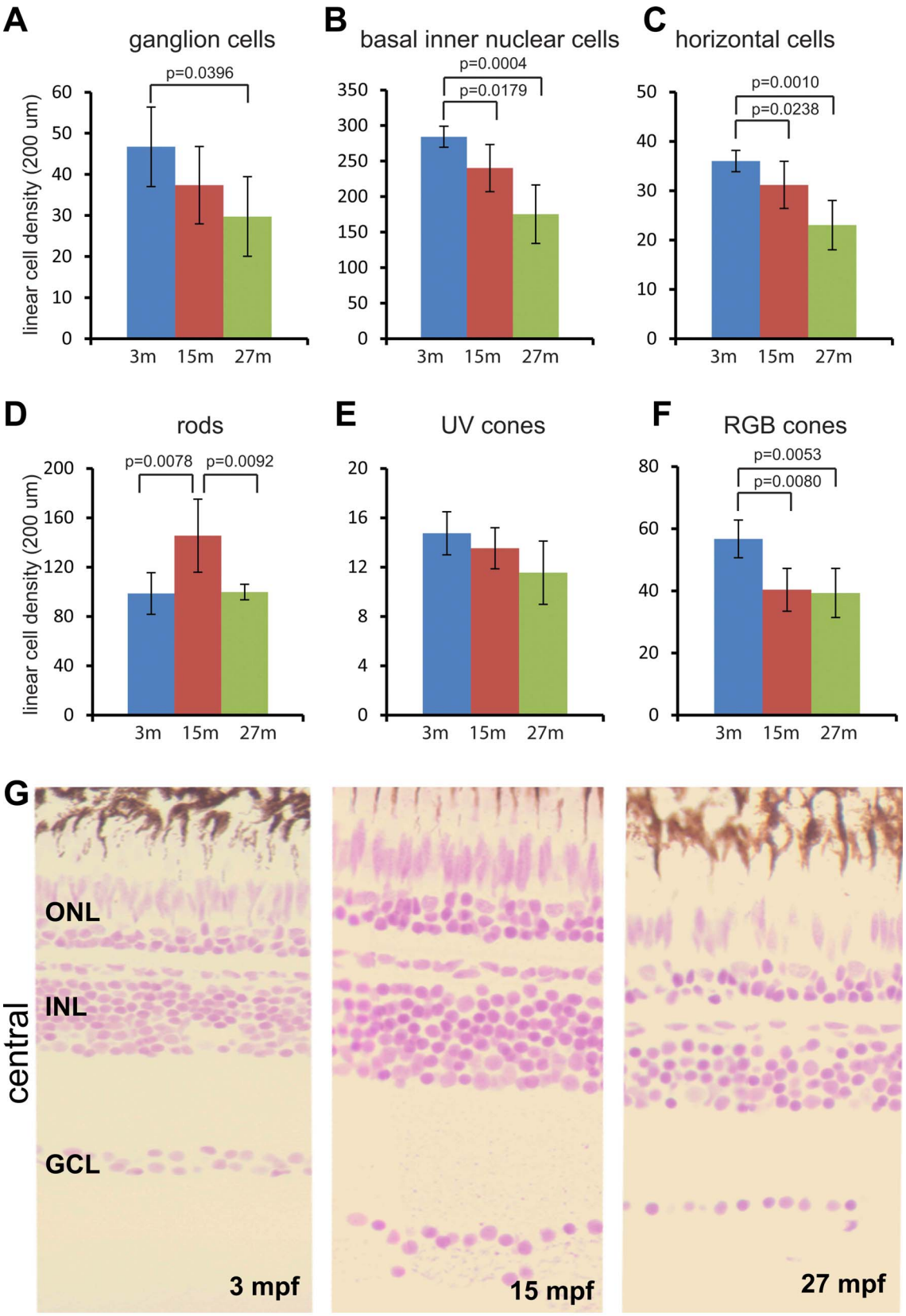

Figure 2. Linear cell density in the central region declines progressively with age, with the exception of rods. (**A–F**) Six cell categories of linear cell density at 3, 15, and 27 mpf. (**A**) Ganglion cells, (**B**) basal inner nuclear cells, (**C**) horizontal cells, (**D**) rods, (**E**) UV cones, and (**F**) RGB cones. Mean ± 1 SD, $n = 5$. (**G**) JB4-Feulgen histology of central retina at 3, 15, and 27 mpf.

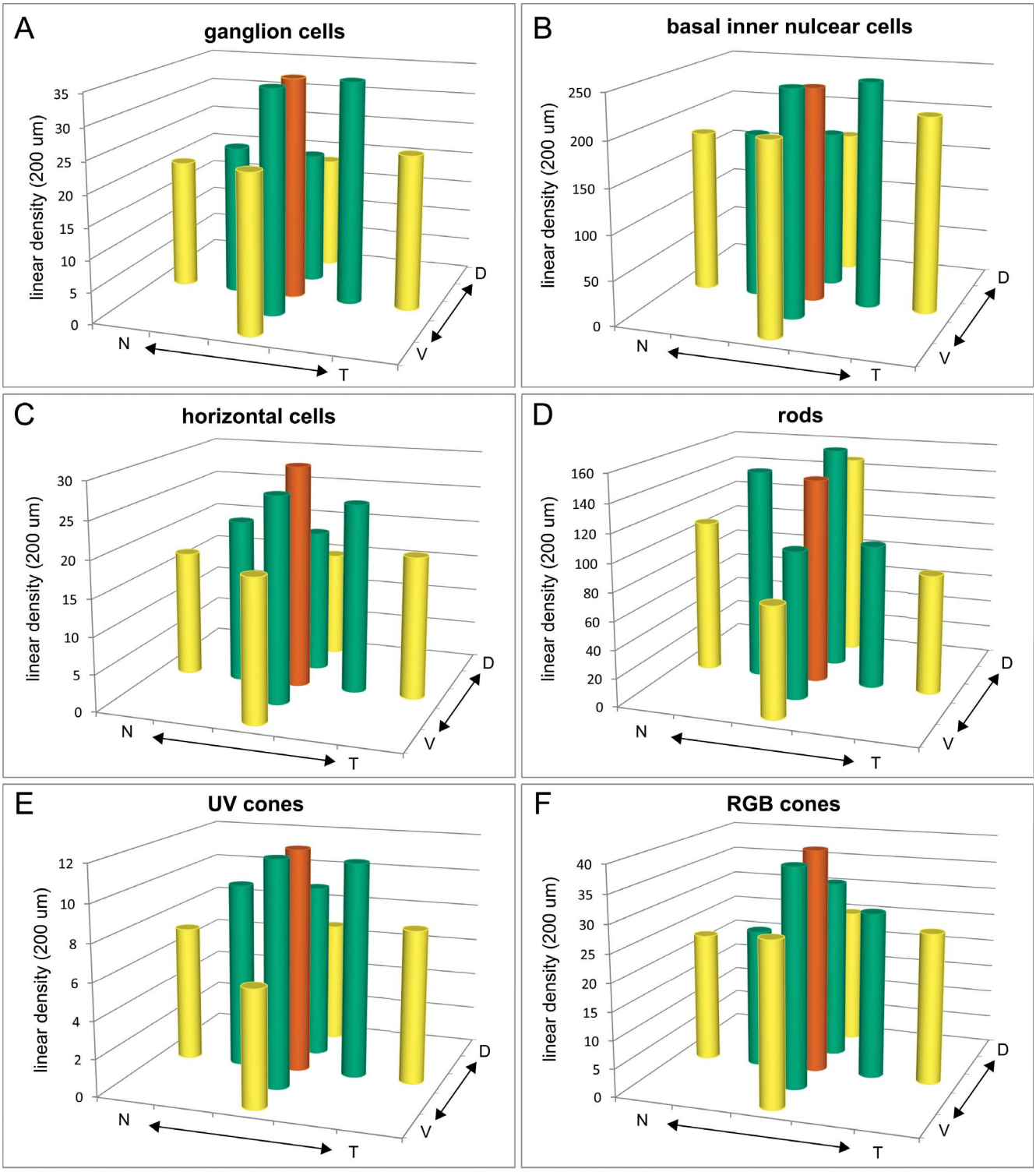

Figure 3. Linear densities of six retinal cell categories vary topographically. (**A–F**) Average linear cell densities in nine sampled regions from five retinas at 15 mpf. (**A**) Ganglion cells, (**B**) basal inner nuclear cells, (**C**) horizontal cells, (**D**) rods, (**E**) UV cones, and (**F**) RGB cones. *Orange bars*, central region; *green bars*, intermediate regions; and *yellow bars*, peripheral regions. N, nasal; T, temporal; V, ventral; D, dorsal.

heads). These morphologic changes indicate that the standard for distinguishing UV cones from RGB cones by their nuclear morphologies would overestimate UV cones and underestimate RGB cones in *pt108b* retina.

In recognition of these limitations, we quantified differential effects of *pt108b* on photoreceptor maintenance with the following simplified criteria/assumptions: (1) round, lightly stained, and apically localized nuclei were counted as UV cone nuclei, recognizing that some of them may have been deformed RGB cones; (2) elongated, lightly stained, and apically localized nuclei were counted as RGB cone nuclei; and (3) round, darkly stained, and basally localized nuclei were

Investigative Ophthalmology & Visual Science

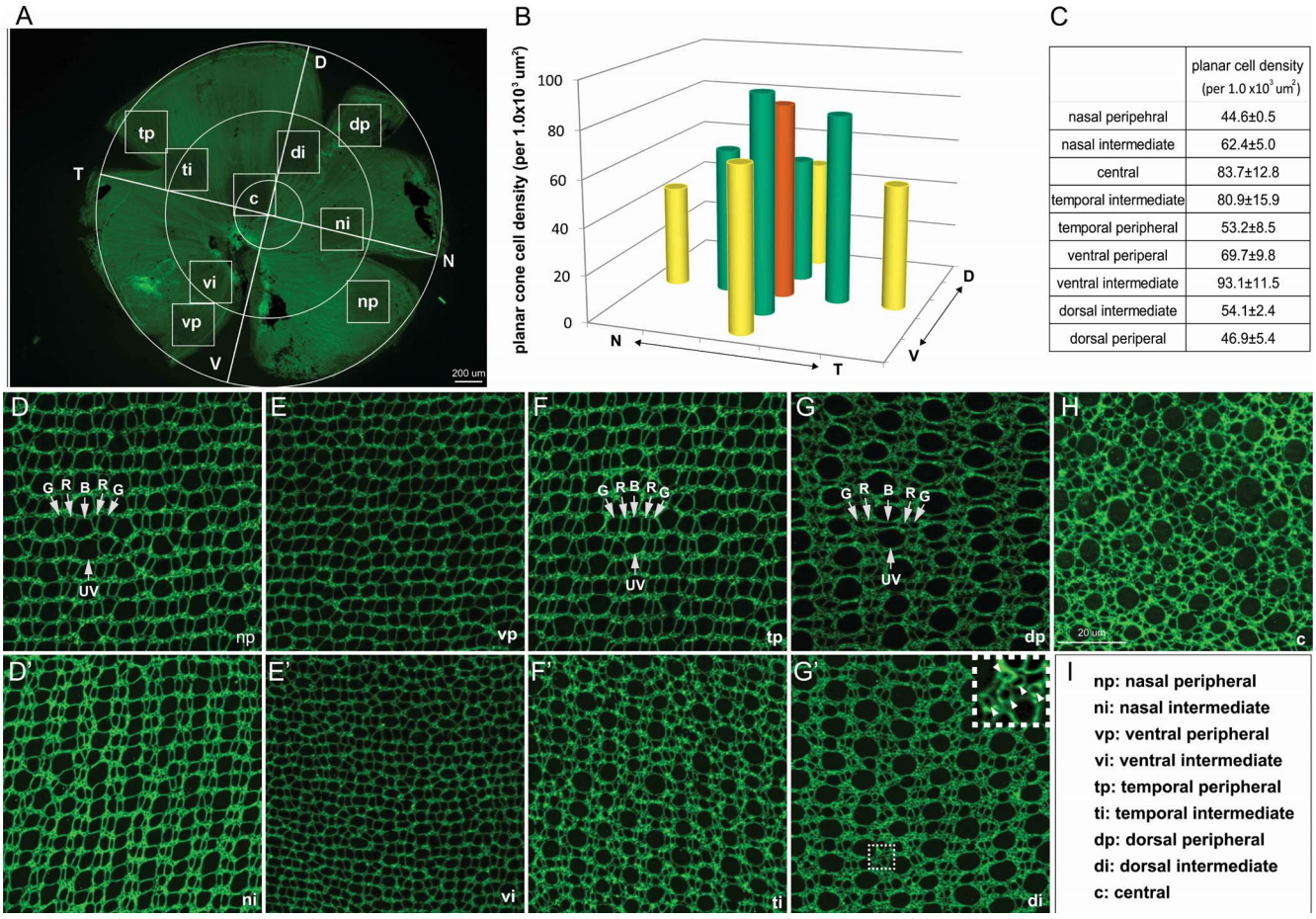

Figure 4. Topographical variations in planar cone densities and sizes. (**A**) Flat-mounted adult zebrafish retina viewed at a low magnification to illustrate the nine sampled regions. (**B**, **C**) Average planar cone densities in nine local regions sampled from retinas at 6 mpf, $n = 3$. (**D–H**) Representative images of ZO-1 immunolabeled apical cell profiles (at the OLM) from the nine local retinal regions. *Arrows* indicate UV cones; R, red cones; G, green cones; and B, blue cones. (**G'**) The inset shows a higher magnification of the boxed region. Round profiles of rods are marked by *arrowheads*. (**I**) Abbreviations of retinal regions.

counted as rod nuclei. With these standards, the overestimation of UV cones (or underestimation of RGB cones) should be very limited in the central retina of aged *pt108b*, because most apically localized and lightly stained round nuclei were UV cone nuclei (Figs. 5C', 5D'). In central retina (Fig. 6A), cell counts indicated that at both 15- and 27-mpf linear density of UV cones in *pt108b* was unchanged, whereas RGB cones were decreased compared with wild-type (Fig. 6B). Loss of RGB cones in *pt108b* was progressive, declining by approximately 50% from 15 to 27 mpf. Overpopulation of rods was seen at 27 mpf (Fig. 6B).

To examine changes in photoreceptor densities in *pt108b* fish in the context of normal aging, we devised a photoreceptor maintenance index to quantify the effects of Crb2b-sf^{EX} on photoreceptor maintenance (Fig. 6C): a positive value suggests enhanced photoreceptor maintenance/addition, and a negative value suggests a net loss of photoreceptors. (The calculation of these indexes measured changes in photoreceptor cell densities between 15 and 27 mpf ages in *pt108b* normalized to wild-type to eliminate any potential developmental effects on production of photoreceptors, thereby revealing only age-related effects on maintenance during this period.) For the central retinal region, the index values clearly demonstrated that Crb2b-sf^{EX} produced selective loss of RGB cones, almost no effect on UV cones, and an overpopulation of rods (Fig. 6D). We applied the same index to the remaining retinal regions, but limited the classification of photoreceptors to rods and cones because it was difficult to distinguish UV cones from the residual RGB cone nuclei, which occurred more frequently in the peripheral and intermediate retinal regions. Similarly, across the *pt108b* retina, Crb2b-sf^{EX} caused rod densities to increase and cone densities to decrease (Supplementary Fig. S7).

Taken together, these data show that secretion of an extracellular fragment of Crb2b in the retina differentially affects photoreceptor maintenance, resulting in overpopulation of rods, no effect on UV cones, but selective death of RGB cones.

Secreted Crb2b-sf^{EX} Changes Planar Cone Patterning

To determine the effect of secreted Crb2b-sf^{EX} on patterning and morphology in the planar dimension, we examined retinal flat-mounts in aged wild-type and *pt108b* fish. The topographic variations in cone sizes observed in young wild-type adults at 6 mpf (Figs. 4D–H) are still present in older adults at 26 mpf, and the stereotypic lattice mosaic pattern of peripheral and intermediate regions is also retained (Figs. 7A–E). In contrast, in aged *pt108b* retinas (18 and 20 mpf), the mosaic patterning of the surviving cones was disrupted in dorsal and nasal regions (Fig. 7A', 7A"–D', 7D"), as reported previously,[22]

Investigative Ophthalmology & Visual Science

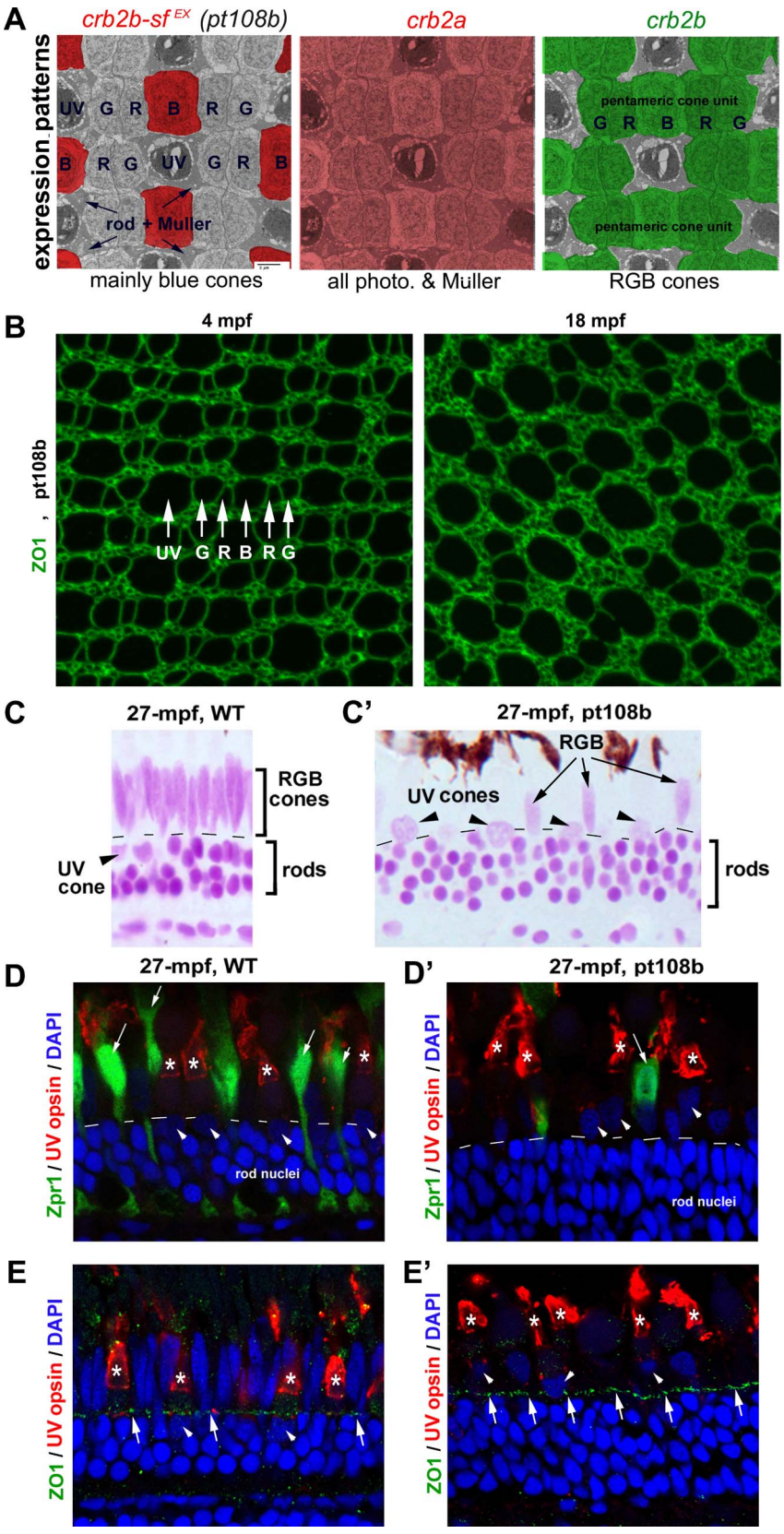

Figure 5. Secreted Crb2b-sf^{EX} affects photoreceptor patterning and maintenance. (**A**) The expression patterns of *Crb* genes are highlighted with different colors superimposed on a transmission electron microscopic image of a tangential section through the photoreceptor layer. The *Crb2b-sf^{EX}* transgene in *pt108b* is mostly expressed in blue cones; endogenous *crb2a* is expressed in all photoreceptors and Müller cells; endogenous *crb2b* is expressed selectively in RGB cones. (**B**) In flat-mount retinal preparations at 4 mpf, ZO-1 immunolabeled apical profiles of photoreceptors in *pt108b* retina form a mosaic pattern, but the regular organization is degraded by 18 mpf. (**C, C'**) JB4-Feulgen staining of retinal cross sections from wild-type

Investigative Ophthalmology & Visual Science

(WT) (**C**) and *pt108* (**C'**) illustrates severe reduction of RGB cones (*arrows*) in *pt108b* retina at 27 mpf, although rods and UV cone nuclei (*arrowheads*) are maintained. *Dashed lines*, OLM. (**D, D'**) In WT retina (**D**) at 27 mpf Zpr1, immunolabeled green and red cones have elongated nuclei (*arrows*), but in *pt108* (**D'**), the nuclei of the few remaining Zpr1-labeled cones are less elongated (*arrow*). UV opsin immunoreactivity (*asterisks*) verified the UV cone identity of nuclei (*arrowheads*) that are abnormally positioned apical to the OLM. DAPI (4′,6-diamidino-2-phenylindole), nuclear stain. *Dashed lines*, OLM. (**E, E'**) ZO1 immunostaining (*arrows*) revealed the OLM, which is positioned apical to the UV cone nuclei in WT (**E**, *arrowheads*) but basal to UV cone nuclei in pt108b (**E'**, *arrowheads*). UV cone outer segments were visualized by UV opsin immunostaining (*asterisks*).

although the patterning defects in temporal-ventral retina were not as severe (Figs. 7E–E"). In dorsal regions with the most disrupted mosaic pattern (Figs. 7C", 7D"), surviving cones were typically rounded, having lost the flattened cone-cone junctions between adjacent cones in the RGB pentamers (compare with RGB cones in Fig. 5A). Accompanying cone loss was an accumulation of rods, which filled the spaces previously occupied by RGB cones (Figs. 7A"–E").

Secreted Crb2b-sf^{EX} Leads to Slow, Progressive Loss of Cones Through Apoptosis

The drastic loss of RGB cones in aged *pt108b* retinas suggests cone death, possibly via apoptosis. To test this hypothesis, we examined 24-mpf wild-type and 19-mpf *pt108b* with flat-mount immunohistochemistry for the apoptosis marker active caspase 3. As predicted, we found active caspase 3–positive apoptotic cells in the photoreceptor layer in *pt108b* fish, especially in the dorsal peripheral region (Figs. 8A–A"', 8B–B"'); by contrast, in wild-type retinas, we did not find active caspase 3 immunoreactivity (Figs. 8C–C"). Examining "cut views" of 3D-reconstructions of whole-mount images to visualize the laminar location of the apoptotic cells (Figs. 8A"', 8B"') shows that active caspase 3-positive cells in the *pt108b* retinas are confined to the layer of photoreceptors at the OLM. These data are consistent with the prediction that cones in aged adult *pt108b* fish die via apoptosis.

Discussion

To gain insight into the roles of Crb proteins in photoreceptor maintenance, we asked whether the *Tg(RH2-2:Crb2b-sf^{EX}/RH2-2:GFP)^{pt108b}* transgenic background not only affects cone-cone adhesion but also affects photoreceptor maintenance in zebrafish. After quantifying normal age-related and topographical changes in retinal cell densities of wild-type zebrafish as a reference, we found that secreted *Crb2b-sf^{EX}*, which interferes with cell adhesion mediated by Crb proteins, differentially affects the maintenance of rods, RGB cones, and UV cones, and suggests that Crb2b may be particularly important for RGB cone survival.

Age-Related and Topographical Variation in Retinal Cell Densities in Zebrafish

As a prerequisite for analyzing Crb proteins in photoreceptor maintenance, we found that linear cell densities of most retinal cell categories, except for rods, decline steadily with age in adult zebrafish. These findings agree with previous observations that retinal growth by stretching reduces densities of retinal cells (except for rod photoreceptors) in other teleost species, such as guppies, African cichlids, and goldfish.[24–27] The initial increase in rod densities in some retinal regions in adult fish from 3 mpf to 15 mpf is consistent with continued generation of rods from Müller glia-derived precursors and rod progenitors and their subsequent intercalation into the photoreceptor layer during the periods when the fish is growing.[38–41] The subsequent stabilization or decline in rod densities at 27 mpf is consistent with the fact that in aged zebrafish, the body and eye growth gradually slows down or stops, and proliferative activity declines.[40,42]

We also showed that cell densities vary topographically across the zebrafish retina. Along the radial dimension, linear cell densities of retinal ganglion cells, horizontal cells, UV cones, and RGB cones are generally higher in the central region than in the peripheral regions. This elevation of cell densities in central retina is similar to observations in other fish, as well as in birds and mammals.[32,43–45] Along the circumferential dimension, rod densities in the dorsal and nasal quadrants of the zebrafish retina are higher, and by contrast, the densities of RGB cones and ganglion cells tend to be higher in the ventral and temporal quadrants. Our findings are consistent with a previous study, which showed by flat-mount imaging that ganglion cells are denser in the ventral and temporal regions than in the nasal and dorsal regions in zebrafish.[46] A higher cone and ganglion cell density in the ventrotemporal retina may represent a retinal specialization corresponding to the part of the visual field located above and in front of the animal, which may be important for predator and prey detection.[47,48]

Crb Proteins Function in Photoreceptor Maintenance

With normal age-related and topographical variations in zebrafish photoreceptor densities as a reference, we found progressive and selective apoptotic death of RGB cones in aged adult *pt108b* fish, with no effect on UV cones, and overpopulation of rods. In young adult *pt108b* fish (4 mpf), retinal structure, lamination, and cone mosaic patterning were all normal, but by 15 mpf, disruption of cone photoreceptor morphology and patterning and loss of RGB cones was apparent in retinal sections as well as retinal flat-mounts. Progressive loss of RGB cones continued to 27 mfp, and the anti-active caspase 3 profiles in the photoreceptor layer suggested that cones were dying via apoptosis. Our quantitative analysis of photoreceptor densities was specifically designed to examine age-related rather than developmental effects, and so we excluded the marginal retina, where new cells are being added to the growing retina. Furthermore, the normal appearance of the retina in young adult *pt108b* fish suggested that photoreceptor differentiation occurred normally. Expression of the Crb2b-sf^{EX} construct was under the control of an opsin promoter, and expression of opsin protein in differentiating photoreceptors is a relatively late developmental event,[36,37] so the initial stages of photoreceptor commitment and differentiation preceed opsin expression. Because production of retinal cells, including photoreceptors, continues in the growing adult retina, newly added cells would be generated in an environment in which Crb2b-sf^{EX} is present. Despite this, the retina appears to develop normally, and the effect on cone photoreceptor maintenance is delayed.

The selective death of RGB cones suggests that Crb2b-sf^{EX} preferentially interferes with function and maintenance of RGB cones. Although the secreted Crb2b-sf^{EX} physically interacts with the broader family of zebrafish Crb proteins (including Crb2a, Crb2b, and Crb1), as suggested previously[22] by in vitro immunoprecipitation analysis (and data not shown), the lack of

Investigative Ophthalmology & Visual Science

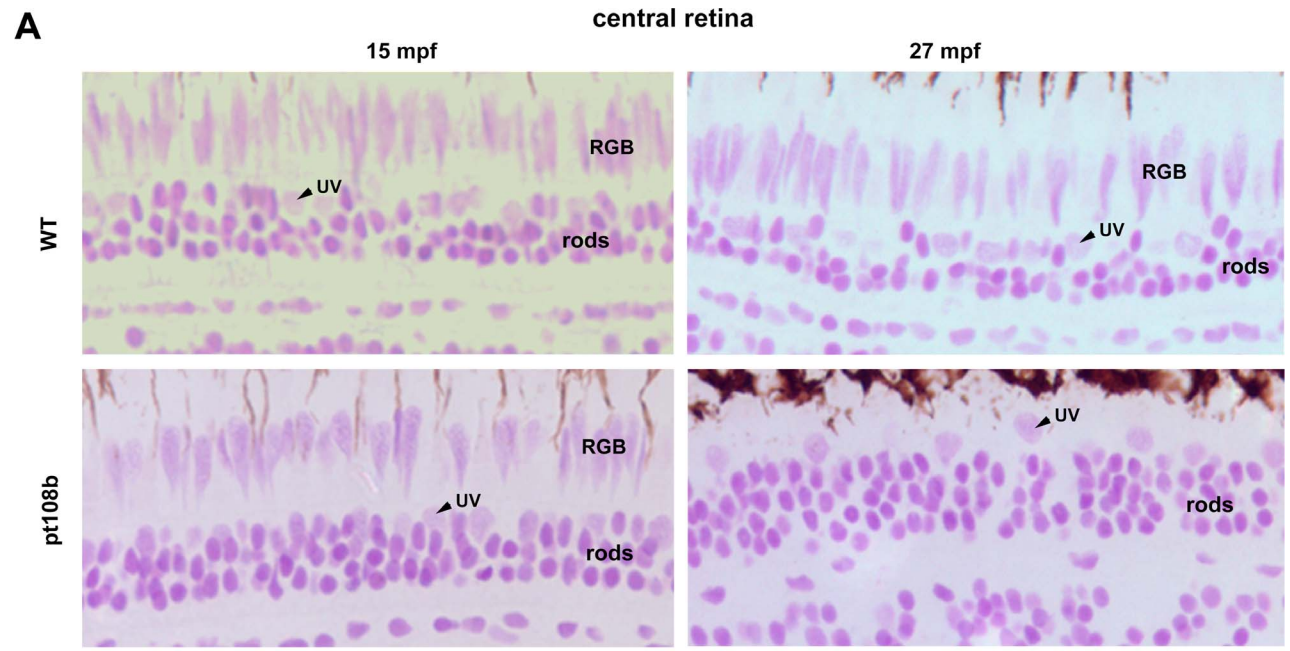

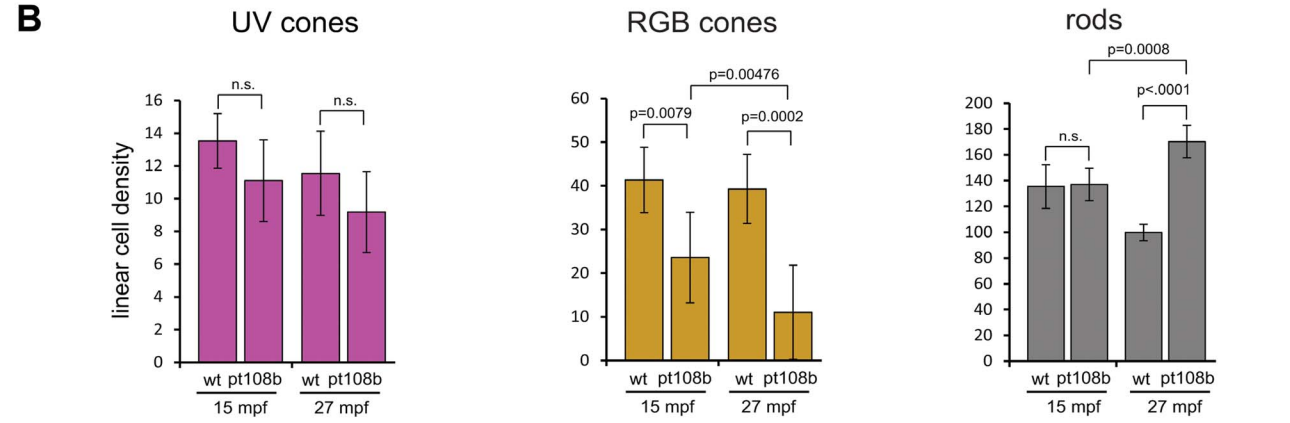

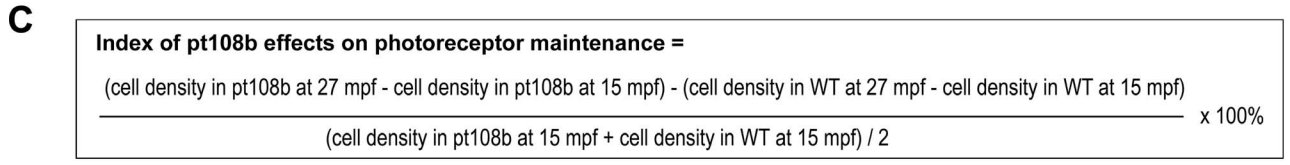

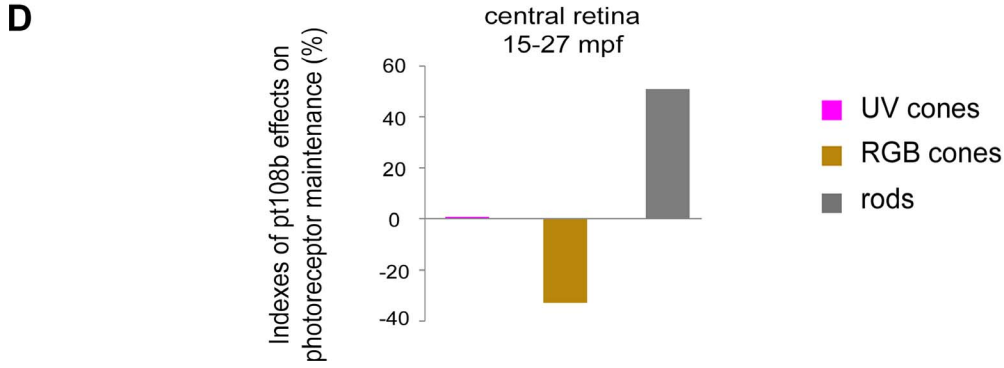

FIGURE 6. Secreted Crb2b-sf^{EX} promotes RGB cone degeneration and rod overpopulation. (**A**) JB4-Feulgen histology illustrates nuclear morphologies and distributions of photoreceptors in the central area of WT and *pt108b* retinas at 15 mpf and 27 mpf. (**B**) Histograms of average linear densities of photoreceptors in central retina of WT and *pt108b* at 15 and 27 mpf. Mean ± 1 SD, $n = 5$. (**C**) Formula for the photoreceptor maintenance index. (**D**) In the central retina in *pt108b*, the photoreceptor maintenance indexes show loss of RGB cones, excess rods, and no effect on UV cones.

Investigative Ophthalmology & Visual Science

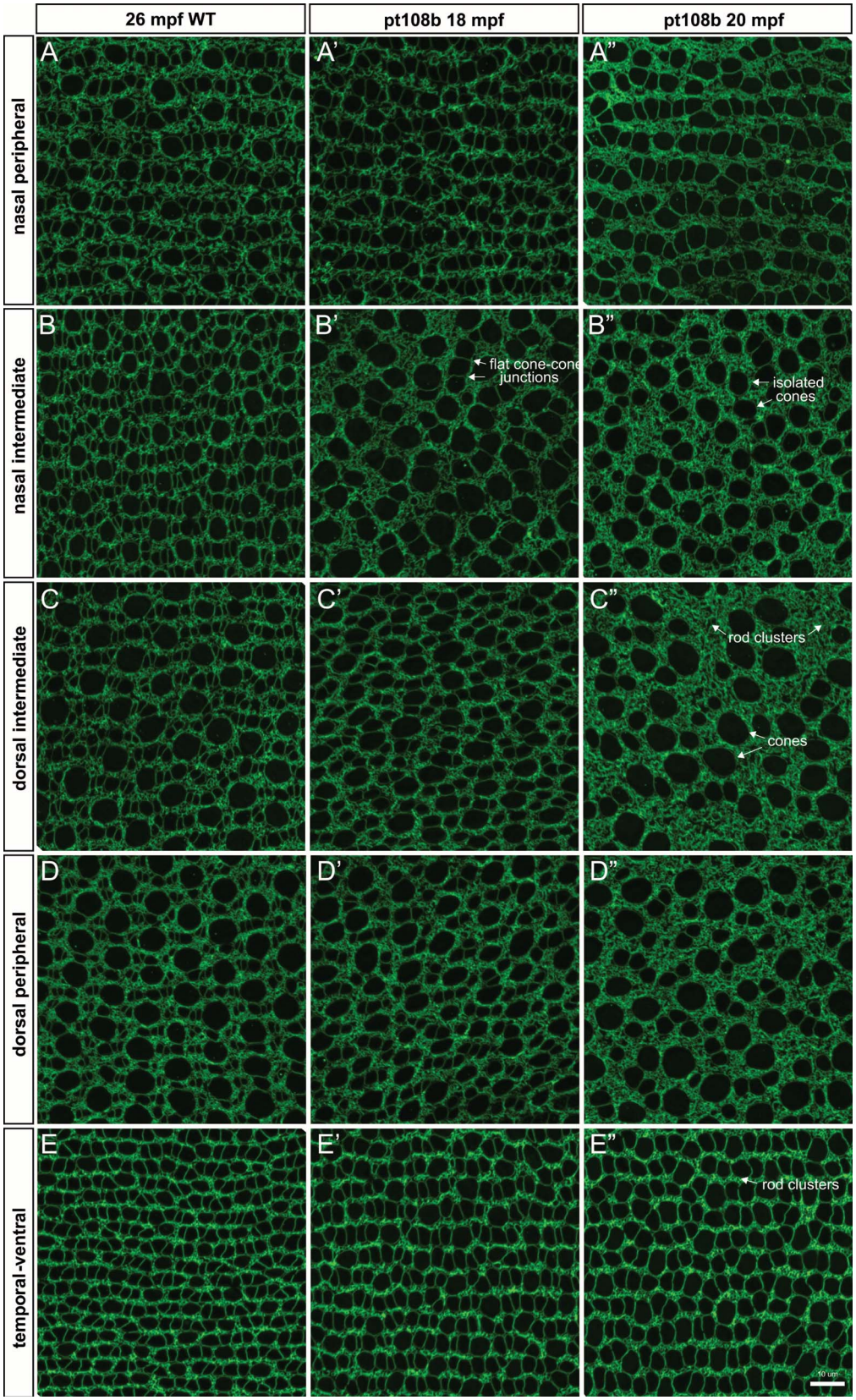

Figure 7. Planar cone density analysis confirmed secreted Crb2b-sf^{EX} produces age-related cone loss. (**A–E**") Comparison of ZO-1 immunolabeled apical cone profiles in representative regions from 26-mpf WT, 18-mpf *pt108b*, and 20-mpf *pt108b* retinas.

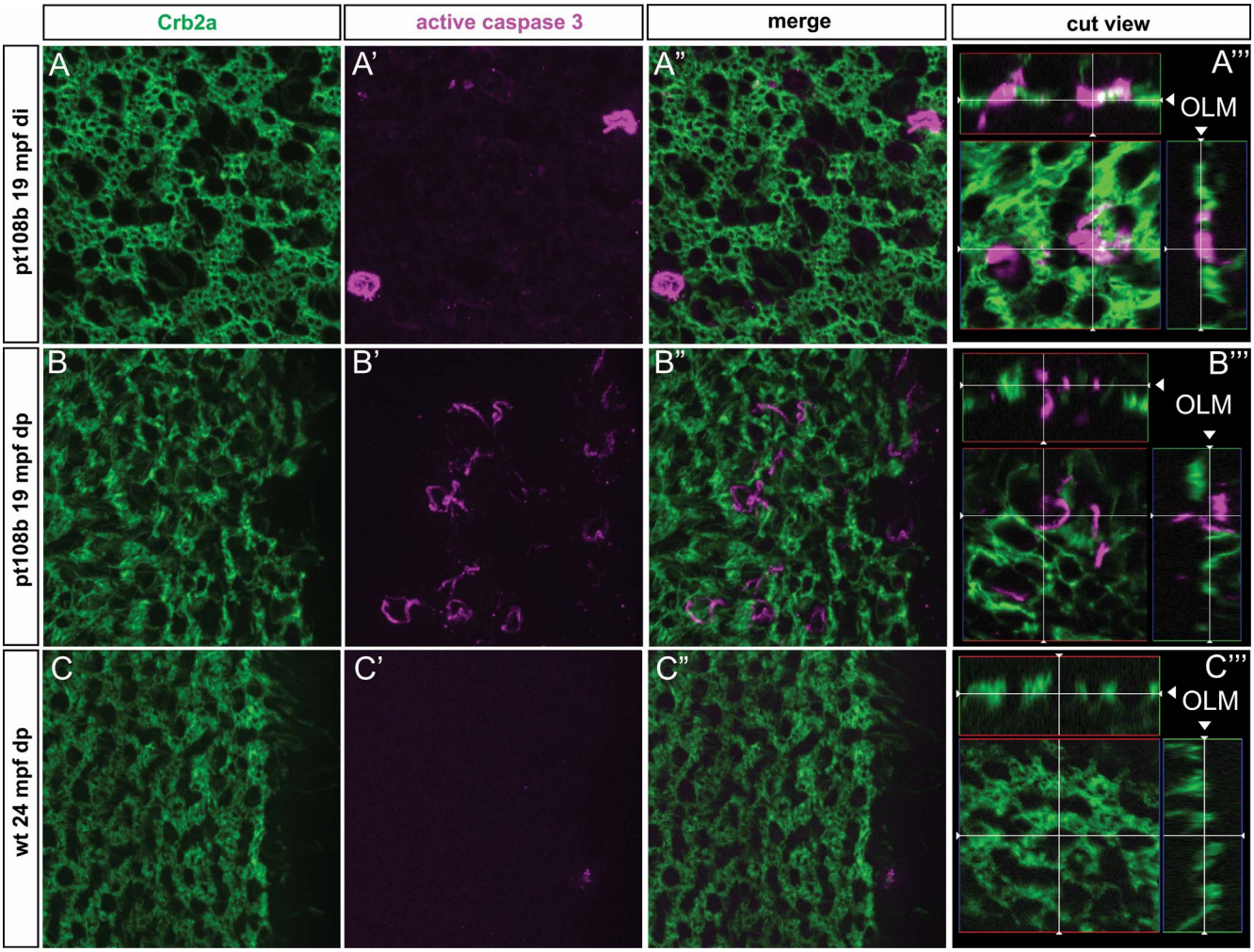

Figure 8. Secreted Crb2b-sf^{EX} induces apoptosis in cones. Retinal flat-mount preparations double-immunolabeled with anti-Crb2a (*green*) and the apoptotic marker, anti-active caspase 3 (*magenta*). (**A**–**A**"', **B**–**B**"') Cells labeled with anti-active caspase 3 were in the photoreceptor layer, as indicated by anti-Crb2a label. (**A**–**A**") and (**B**–**B**") represent 2D planar views, and (**A**"') and (**B**"') include 3D-reconstructed "cut views" (in the *xz* and *xy* planes) at the level of the OLM, indicated by the *white cross hairs*, demonstrating that apoptotic and photoreceptor-specific labels are in the photoreceptor layer. (**C**–**C**"') Active caspase 3–labeled photoreceptors were not observed in WT retinas.

an effect on UV cones suggests that Crb2b-sf^{EX} interference with Crb2a- and Crb1-mediated mechanisms may not be consequential for photoreceptor maintenance. If this interpretation is correct, the overpopulation of rods may be simply a secondary effect of normal mechanisms of growth-related rod photoreceptor production in the teleost retina.[41] For example, we previously reported overproduction of rods in light-damaged zebrafish retinas with selective loss of UV cones.[30] Nevertheless, we cannot rule out the possibility that in *pt108b*, Crb2b-sf^{EX} interference with Crb2a, which is expressed by both rods and Müller glia,[22] may directly promote rod overpopulation.

The selective death of RGB cones is observed only in older adults. This slow, progressive degeneration may be the reason why Müller glial cells were not stimulated to regenerate lost RGB cones, as has been reported previously in a zebrafish genetic model of rod degeneration in which loss of rods was neither extensive nor acute.[49] In line with the observation that cones can survive when rods degenerate in zebrafish,[50,51] the opposite fates of rods and cones in *pt108b* supports the notion that the maintenance of rods and cones is regulated differently and their survival is not interdependent in zebrafish.

The selective death of cone subtypes has not been observed in genetic mouse models that affect a single *Crb* gene.[10] Although mutations in the human *CRB1* gene can cause severe retinal dystrophies, loss of *Crb1* in mice (including the spontaneous *rd8* mutation and *Crb1* knockout) show a relatively mild phenotype, with focal regions of photoreceptor disorganization, whereas conditional knockout of *Crb2* in mice has a more severe and progressive retinal degeneration phenotype that more closely models human disease.[10] Based on molecular phylogeny of opsins, zebrafish red cones, among the cone subtypes lost in *pt108b*, are the homolog of mammalian L/M cones; by contrast, the UV cones, persistent in *pt108b*, are homologous to mammalian S cones.[52] Thus, the *pt108b* zebrafish line, which targets Crb2b function, provides a useful new tool to investigate the mechanisms of Crb proteins in photoreceptor maintenance and survival.

Although the downstream molecular pathways of Crb2b regulation in zebrafish photoreceptors are yet to be determined, one possible target is the Hippo signaling pathway.[10] Crb is known to activate the Hippo kinase cascade that phosphorylates and inhibits the transcription cofactor YAP/TAZ, which is required for diverse biological functions, including cell proliferation as well as apoptosis, depending

on cellular context.[53–56] It is tempting to speculate that Crb2b may regulate Hippo signaling to promotes RGB cone maintenance.

Acknowledgments

The authors thank Yuande Zhang (the First Hospital of Jilin University) and Ying Wang (the Second Hospital of Jilin University) for helping with paraffin histology.

Supported by National Science Foundation (NSF) Grant IOS1353914 (PAR) and Natural Science Foundation of China (NSFC) Grant 81400433 (JF); National Institutes of Health Grants EY016099, EY025638 (XW), and P30 EY08098; a grant from the Eye and Ear Foundation of Pittsburgh; an unrestricted grant from Research to Prevent Blindness; the Norman Bethune Program of Jilin University (2105306) (JF); and The Training Program for Outstanding Young Teachers of Jilin University (419080500588) (JF).

Disclosure: **J. Fu**, None; **M. Nagashima**, None; **C. Guo**, None; **P.A. Raymond**, None; **X. Wei**, None

References

1. Pacione LR, Szego MJ, Ikeda S, Nishina PM, McInnes RR. Progress toward understanding the genetic and biochemical mechanisms of inherited photoreceptor degenerations. *Annu Rev Neurosci*. 2003;26:657–700.
2. Weleber RG. Inherited and orphan retinal diseases: phenotypes, genotypes, and probable treatment groups. Proceedings of the First International Symposium on Translational Clinical Research for Inherited and Orphan Retinal Diseases. November 5–7, 2004. Washington, DC, USA. *Retina*. 2005;25: S4–S7.
3. Hartong DT, Berson EL, Dryja TP. Retinitis pigmentosa. *Lancet*. 2006;368:1795–1809.
4. den Hollander AI, Davis J, van der Velde-Visser SD, et al. CRB1 mutation spectrum in inherited retinal dystrophies. *Hum Mutat*. 2004;24:355–369.
5. den Hollander AI, Roepman R, Koenekoop RK, Cremers FP. Leber congenital amaurosis: genes, proteins and disease mechanisms. *Prog Retin Eye Res*. 2008;27:391–419.
6. Bulgakova NA, Knust E. The Crumbs complex: from epithelial-cell polarity to retinal degeneration. *J Cell Sci*. 2009;122:2587–2596.
7. Bujakowska K, Audo I, Mohand-Said S, et al. CRB1 mutations in inherited retinal dystrophies. *Hum Mutat*. 2012;33:306–315.
8. Beryozkin A, Zelinger L, Bandah-Rozenfeld D, et al. Mutations in CRB1 are a relatively common cause of autosomal recessive early-onset retinal degeneration in the Israeli and Palestinian populations. *Invest Ophthalmol Vis Sci*. 2013;54:2068–2075.
9. Ehrenberg M, Pierce EA, Cox GF, Fulton AB. CRB1: one gene, many phenotypes. *Semin Ophthalmol*. 2013;28:397–405.
10. Alves CH, Pellissier LP, Wijnholds J. The CRB1 and adherens junction complex proteins in retinal development and maintenance. *Prog Retin Eye Res*. 2014;40:35–52.
11. Tepass U, Theres C, Knust E. Crumbs encodes an EGF-like protein expressed on apical membranes of Drosophila epithelial cells and required for organization of epithelia. *Cell*. 1990;61:787–799.
12. Pocha SM, Knust E. Complexities of Crumbs function and regulation in tissue morphogenesis. *Curr Biol*. 2013;23:R289–R293.
13. Thompson BJ, Pichaud F, Roper K. Sticking together the Crumbs—an unexpected function for an old friend. *Nat Rev Mol Cell Biol*. 2013;14:307–314.
14. Pellikka M, Tanentzapf G, Pinto M, et al. Crumbs, the *Drosophila* homologue of human CRB1/RP12, is essential for photoreceptor morphogenesis. *Nature*. 2002;416:143–149.
15. Izaddoost S, Nam SC, Bhat MA, Bellen HJ, Choi KW. *Drosophila* Crumbs is a positional cue in photoreceptor adherens junctions and rhabdomeres. *Nature*. 2002;416:178–183.
16. den Hollander AI, ten Brink JB, de Kok YJ, et al. Mutations in a human homologue of Drosophila crumbs cause retinitis pigmentosa (RP12). *Nat Genet*. 1999;23:217–221.
17. van den Hurk JA, Rashbass P, Roepman R, et al. Characterization of the Crumbs homolog 2 (CRB2) gene and analysis of its role in retinitis pigmentosa and Leber congenital amaurosis. *Mol Vis*. 2005;11:263–273.
18. Richard M, Roepman R, Aartsen WM, et al. Toward understanding CRUMBS function in retinal dystrophies. *Hum Mol Genet*. 2006;15(Spec No 2):R235–R243.
19. Gosens I, den Hollander AI, Cremers FP, Roepman R. Composition and function of the Crumbs protein complex in the mammalian retina. *Exp Eye Res*. 2008;86:713–726.
20. Pellissier LP, Quinn PM, Alves CH, et al. Gene therapy into photoreceptors and Müller glial cells restores retinal structure and function in CRB1 retinitis pigmentosa mouse models. *Hum Mol Genet*. 2015;24:3104–3118.
21. Omori Y, Malicki J. Oko meduzy and related crumbs genes are determinants of apical cell features in the vertebrate embryo. *Curr Biol*. 2006;16:945–957.
22. Zou J, Wang X, Wei X. Crb apical polarity proteins maintain zebrafish retinal cone mosaics via intercellular binding of their extracellular domains. *Dev Cell*. 2012;22:1261–1274.
23. Fang W, Guo C, Wei X. Rainbow enhancers regulate restrictive transcription in teleost green, red, and blue cones. *J Neurosci*. 2017;37:2834–2848.
24. Müller H. Bau und Wachstum der Netzhaut des Guppy (*Lebistes reticulatus*) [in German]. *Zoologische Jahrbuch*. 1952;63:275–324.
25. Ali MA. Stretching of the retina during growth of salmon (*Salmo salar*). *Growth*. 1964;28:83–89.
26. Johns PR. Growth of the adult goldfish eye. II. Increase in retinal cell number. *J Comp Neurol*. 1977;176:331–341.
27. Fernald RD. Teleost vision: seeing while growing. *J Exp Zool*. 1990;(Suppl 5):167–180.
28. Vihtelic TS, Doro CJ, Hyde DR. Cloning and characterization of six zebrafish photoreceptor opsin cDNAs and immunolocalization of their corresponding proteins. *Vis Neurosci*. 1999;16:571–585.
29. Fu J, Fang W, Zou J, et al. A robust procedure for distinctively visualizing zebrafish retinal cell nuclei under bright field light microscopy. *J Histochem Cytochem*. 2013;61:248–256.
30. Raymond PA, Colvin SM, Jabeen Z, et al. Patterning the cone mosaic array in zebrafish retina requires specification of ultraviolet-sensitive cones. *PLoS One*. 2014;9:e85325.
31. Johns PR. Growth of fish retinas. *Am Zool*. 1981;21:447–458.
32. Mastronarde DN, Thibeault MA, Dubin MW. Non-uniform postnatal growth of the cat retina. *J Comp Neurol*. 1984;228: 598–608.
33. Morris VB, Wylie CC, Miles VJ. The growth of the chick retina after hatching. *Anat Rec*. 1976;184:111–113.
34. Straznicky C, Hiscock J. Post-metamorphic retinal growth in *Xenopus*. *Anat Embryol (Berl)*. 1984;169:103–109.
35. Packer O, Hendrickson AE, Curcio CA. Development redistribution of photoreceptors across the *Macaca nemestrina* (pigtail macaque) retina. *J Comp Neurol*. 1990;298:472–493.
36. Salbreux G, Barthel LK, Raymond PA, Lubensky DK. Coupling mechanical deformations and planar cell polarity to create regular patterns in the zebrafish retina. *PLoS Comput Biol*. 2012;8:e1002618.

37. Allison WT, Barthel LK, Skebo KM, Takechi M, Kawamura S, Raymond PA. Ontogeny of cone photoreceptor mosaics in zebrafish. *J Comp Neurol*. 2010;518:4182–4195.
38. Raymond PA, Rivlin PK. Germinal cells in the goldfish retina that produce rod photoreceptors. *Dev Biol*. 1987;122:120–138.
39. Otteson, DC, Hitchcock PF. Stem cells in the teleost retina: persistent neurogenesis and injury-induced regeneration. *Vision Res*. 2003;43:927–936.
40. Bernardos RL, Barthel LK, Meyers JR, Raymond PA. Late-stage neuronal progenitors in the retina are radial Müller glia that function as retinal stem cells. *J Neurosci*. 2007;27:7028–7040.
41. Stenkamp DL. The rod photoreceptor lineage of teleost fish. *Prog Retin Eye Res*. 2011;30:395–404.
42. Marcus RC, Delaney CL, Easter SS Jr. Neurogenesis in the visual system of embryonic and adult zebrafish (*Danio rerio*). off. *Vis Neurosci*. 1999;16:417–424.
43. Dalton BE, de Busserolles F, Marshall NJ, Carleton KL. Retinal specialization through spatially varying cell densities and opsin coexpression in cichlid fish. *J Exp Biol*. 2017;220:266–277.
44. Stone J, Rapaport DH, Williams RW, Chalupa L. Uniformity of cell distribution in the ganglion cell layer of prenatal cat retina: implications for mechanisms of retinal development. *Brain Res*. 1981;254:231–242.
45. Chen Y, Naito J. A quantitative analysis of cells in the ganglion cell layer of the chick retina. *Brain Behav Evol*. 1999;53:75–86.
46. Mangrum WI, Dowling JE, Cohen ED. A morphological classification of ganglion cells in the zebrafish retina. *Vis Neurosci*. 2002;19:767–779.
47. Beaudet L, Novales Flamarique I, Hawryshyn CW. Cone photoreceptor topography in the retina of sexually mature Pacific salmonid fishes. *J Comp Neurol*. 1997;383:49–59.
48. Temple SE. Why different regions of the retina have different spectral sensitivities: a review of mechanisms and functional significance of intraretinal variability in spectral sensitivity in vertebrates. *Vis Neurosci*. 2011;28;281–293.
49. Montgomery JE, Parsons MJ, Hyde DR. A novel model of retinal ablation demonstrates that the extent of rod cell death regulates the origin of the regenerated zebrafish rod photoreceptors. *J Comp Neurol*. 2011;518:800–814.
50. Morris AC, Schroeter EH, Bilotta J, Wong RO, Fadool JM. Cone survival despite rod degeneration in XOPS-mCFP transgenic zebrafish. *Invest Ophthalmol Vis Sci*. 2005;46:4762–4771.
51. Vihtelic TS, Soverly JE, Kassen SC, Hyde DR. Retinal regional differences in photoreceptor cell death and regeneration in light-lesioned albino zebrafish. *Exp Eye Res*. 2006;82:558–575.
52. Yokoyama S. Molecular evolution of vertebrate visual pigments. *Prog Retin Eye Res*. 2000;19:385–419.
53. Pan D. The Hippo signaling pathway in development and cancer. *Dev Cell*. 2010;19:491–505.
54. Yu FX, Guan KL. The Hippo pathway: regulators and regulations. *Genes Dev*. 2013;27:355–371.
55. Elbediwy A, Vincent-Mistiaen ZI, Thompson BJ. YAP and TAZ in epithelial stem cells: a sensor for cell polarity, mechanical forces and tissue damage. *Bioessays*. 2016;38:644–653.
56. Meng Z, Moroishi T, Guan KL. Mechanisms of Hippo pathway regulation. *Genes Dev*. 2016;30:1–17.

Investigative Ophthalmology & Visual Science